A wavenumber approach to quantifying the isotropy of the sound field in reverberant spaces

Nolan, Melanie; Fernandez Grande, Efren; Brunskog, Jonas; Jeong, Cheol-Ho

Published in:
Journal of the Acoustical Society of America

Link to article, DOI:
10.1121/1.5032194

Publication date:
2018

Document Version
Publisher's PDF, also known as Version of record

A wavenumber approach to quantifying the isotropy of the sound field in reverberant spaces

Mélanie Nolan, Efren Fernandez-Grande, Jonas Brunskog, and Cheol-Ho Jeong

Citation: The Journal of the Acoustical Society of America **143**, 2514 (2018); doi: 10.1121/1.5032194
View online: https://doi.org/10.1121/1.5032194
View Table of Contents: http://asa.scitation.org/toc/jas/143/4
Published by the Acoustical Society of America

A wavenumber approach to quantifying the isotropy of the sound field in reverberant spaces[a)]

Mélanie Nolan,[b)] Efren Fernandez-Grande, Jonas Brunskog, and Cheol-Ho Jeong
Acoustic Technology, Department of Electrical Engineering, Technical University of Denmark (DTU), Building 352, Ørsteds Plads, DK-2800 Kongens Lyngby, Denmark

(Received 1 August 2017; revised 10 March 2018; accepted 29 March 2018; published online 27 April 2018)

This study proposes an experimental method for evaluating isotropy in enclosures, based on an analysis of the wavenumber spectrum in the spherical harmonics domain. The wavenumber spectrum, which results from expanding an arbitrary sound field into a plane-wave basis, is used to characterize the spatial properties of the observed sound field. Subsequently, the obtained wavenumber spectrum is expanded into a series of spherical harmonics, and the moments from this spherical expansion are used to characterize the isotropy of the wave field. The analytical framework is presented. The method is examined numerically and experimentally, based on array measurements in four chambers: two anechoic chambers (one with a single source and another with an array of 52 sources), a reverberation chamber, and the same reverberation chamber with a sample of absorbing material on the floor. The results indicate that the proposed methodology is suitable for assessing the isotropy of a sound field. © *2018 Acoustical Society of America*. https://doi.org/10.1121/1.5032194

[FM] Pages: 2514–2526

I. INTRODUCTION

Many acoustical measurements rely on the assumption that the sound field is *diffuse*. Examples include standardized measurements of sound absorption and transmission loss in reverberation rooms.[1,2] The diffuse sound field is yet an idealized concept, and the sound field in any reverberant space differs in fundamental aspects from the perfectly diffuse sound field.[3,4] It is therefore of interest to examine the behavior of sound fields in real rooms, and the concept of acoustic diffusion in a room.

Various models of diffuse sound fields have been described in the literature.[3–6] The conception that any complex sound field can be defined as the superposition of a set of plane waves is used as a starting point for a model referred to as the *random wave model*, which theory is essentially due to Schroeder,[7] Waterhouse,[8] Lubman,[9] Jacobsen,[4,10,11] and Pierce.[12] The diffuse sound field is described as composed of plane waves with random phases and equal magnitudes, which directions of propagation are uniformly distributed over all angles of incidence, such that the same amount of energy arrives at the observation point from each element of solid angle. Since infinitely many plane waves are assumed, this model is idealized, but gives a good approximation to the sound field in a reverberation room driven with a pure tone in the frequency range where the modal overlap is high (typically above Schroeder's frequency). In this study, we associate the concept of diffusion with this theory.

Different methods have been proposed for evaluating the degree of diffusion in a room. Cook *et al.*[13] (and later Bodlund[14]), examined the cross-correlation between pressure measurements at neighboring positions. The core idea behind this approach is that, in a perfectly diffuse sound field, the cross-correlation function between two omnidirectional microphones follows a sinc function pattern. In Ref. 15, Jacobsen and Roisin presented a method of determining spatial correlation functions in a room, suitable to other quantities than the sound pressure. Noteworthy and perhaps overlooked is the work by Ebeling,[16] who interpreted the cross-correlation function derived by Cook *et al.*[13] in the spatial frequency domain. Subsequently, he proposed a multipole expansion of the spatial correlation function leading to a measure for *spatial diffusivity*. More recently, other methods have investigated how spherical microphone arrays can be used to characterize diffuseness. Gover *et al.*[17] estimate the directional impulse responses of a room using a spherical array beamformer, to evaluate the distribution of acoustic energy arriving to the array from different directions. Following a different approach, Epain and Jin[18] analyze the spherical harmonic covariance matrix to estimate diffuseness arising from the presence of multiple uncorrelated sources. Yet, other measures have been proposed, consisting in measuring the acoustic intensity over time,[19–24] or the acoustic energy at various points across space.[25]

From the standpoint of the random wave theory, sound field diffusion relies on two essential features: (i) the directions of propagation of the plane waves that conform the sound field must be uniformly distributed over all angles of incidence (i.e., isotropic sound field), and (ii) these plane waves must have random relative phases. This publication is strictly concerned with quantifying sound field isotropy [i.e., condition (i)].

An experimental method for evaluating isotropy in enclosures is proposed that is based on an analysis of the wavenumber spectrum in the spherical harmonics domain.

[a)]Portions of this work were presented in "A wavenumber approach to characterizing the diffuse field conditions in reverberation rooms," Proceedings of the 22nd International Congress on Acoustics, Buenos Aires, Argentina, September 2016.

[b)]Electronic mail: melnola@elektro.dtu.dk

 0001-4966/2018/143(4)/2514/13/$30.00

On the one hand, the wavenumber spectrum characterizes the magnitudes of the sound waves arriving from definite directions at the observation point.[26] On the other hand, a spherical harmonic basis is best suited to analyze isotropy, as it depends only on direction (polar and azimuth angles), and can provide an unequivocal characterization of the symmetry of a given quantity. Hence, the use of spherical harmonics as a basis for describing isotropy is commonly used in several areas of physics.[27–30] In this work, we propose to use a spherical harmonic expansion on the wavenumber spectrum, the underlying hypothesis being that in a perfectly isotropic sound field, the wavenumber spectrum is rotationally symmetric. Because the spherical harmonic expansion is performed on the wavenumber spectrum, and not on the recorded pressure signals directly,[18,29,30] the proposed method is not restricted to measurements with a spherical array or other geometry. The method is valid for uniform or random spatial sampling, as opposed to Refs. 17 and 18. Besides, the analytical framework proposed in this paper is far simpler than the theory developed in Ref. 16, in that it considers the actual pressure field directly, rather than its ensemble statistics and spatial correlation. Consequently, the proposed methodology is valid even when the random wave theory no longer holds (this would be the case at low frequencies or when absorbing material is spread over one or several surfaces).

The present paper is organized as follows: the theoretical background is presented in Sec. II, and the validity of the method is evaluated in Secs. III and IV, based on a numerical and an experimental study using array measurements.

II. THEORETICAL BACKGROUND

A. Wavenumber spectrum

We consider the steady-state sound field produced by a pure-tone source in a reverberation chamber. The resulting sound field at the point characterized by the vector $\mathbf{r}_m = (x_m, y_m, z_m)$ can be represented as a superposition of plane waves, each traveling in a direction specified by the wavenumber vector $\mathbf{k} = (k_x, k_y, k_z)$. Each plane wave may have different amplitudes and phases, which we account for by using a complex coefficient term $P(k_x, k_y, k_z) = P(\mathbf{k})$,

$$p(\mathbf{r}_m) = \int_{-\infty}^{+\infty}\int\int P(\mathbf{k}) e^{-j(k_x x + k_y y + k_z z)} d\mathbf{k}. \tag{1}$$

The integrals represent a three-dimensional inverse Fourier transform in k_x, k_y, and k_z, respectively, which guarantees that any pressure distribution may be represented by Eq. (1). The quantity $P(\mathbf{k}) = |P(\mathbf{k})| e^{j\phi(\mathbf{k})}$ is the wavenumber spectrum, with $|P(\mathbf{k})|$ and $\phi(\mathbf{k})$ its magnitude and phase, respectively. We must keep in mind that all propagating plane waves satisfy the condition $\|\mathbf{k}\|^2 = k^2 = k_x^2 + k_y^2 + k_z^2$ with $k^2 \geq k_x^2 + k_y^2$ (indicating that evanescent waves are not present). Introducing spherical coordinates, $x_m = r \sin\vartheta \cos\varphi$, $y_m = r \sin\vartheta \sin\varphi$, $z_m = r\cos\vartheta$ and $k_x = k \sin\theta\cos\phi$, $k_y = k\sin\theta\sin\phi$, $k_z = k\cos\theta$, Eq. (1) becomes

$$p(\mathbf{r}_m) = \int_0^{+\infty}\int_0^{2\pi}\int_0^{\pi} P(\mathbf{k}) e^{-jkr(\sin\theta\sin\vartheta\cos(\phi-\varphi)+\cos\theta\cos\vartheta)} \times k^2 \sin\theta dk d\theta d\phi. \tag{2}$$

Since we are interested in the sound field produced by a pure-tone with frequency f_0, all propagating waves should appertain to the surface of the *radiation sphere* of radius $k_0 = 2\pi f_0/c$ in the wavenumber domain. In other words, the wavenumber spectrum $P(\mathbf{k})$ must only consist of components that fulfill

$$P(k,\theta,\phi) = \frac{\delta(k-k_0)}{4\pi k^2}\tilde{P}(\theta,\phi), \tag{3}$$

where $\delta(k-k_0)/4\pi k^2$ corresponds to the Dirac delta function in spherical coordinates with symmetry with respect to both θ and ϕ. $\tilde{P}(\theta,\phi)$ denotes the two-dimensional wavenumber spectrum expressed in spherical coordinates. Combining Eqs. (2) and (3) yields

$$p(r,\vartheta,\varphi) = \frac{1}{4\pi}\int_0^{2\pi}\int_0^{\pi}\tilde{P}(\theta,\phi) e^{-jk_0 r(\sin\theta\sin\vartheta\cos(\phi-\varphi)+\cos\theta\cos\vartheta)} \times \sin\theta d\theta d\phi. \tag{4}$$

The pressure distribution measured over a surface associated with $\mathbf{r}_m = (a,\vartheta,\varphi)$, can now be represented by

$$p(a,\vartheta,\varphi) = \frac{1}{4\pi}\int_0^{2\pi}\int_0^{\pi}\tilde{P}(\theta,\phi) e^{-jk_0 a(\sin\theta\sin\vartheta\cos(\phi-\varphi)+\cos\theta\cos\vartheta)} \times \sin\theta d\theta d\phi, \tag{5}$$

where a spherical measurement area of radius a is chosen. The two-dimensional inverse Fourier transformation required for explicitly calculating $\tilde{P}(\theta,\phi)$ reads

$$\tilde{P}(\theta,\phi) = \pi\int_0^{2\pi}\int_0^{\pi} p(a,\vartheta,\varphi) e^{jk_0 a(\sin\theta\sin\vartheta\cos(\phi-\varphi)+\cos\theta\cos\vartheta)} \times \sin\vartheta d\vartheta d\varphi. \tag{6}$$

In practice, no assumption whatsoever concerning the shape of the measurement area is necessary, since the analysis is done via discrete Fourier transforms, based on a discrete approximation of Eq. (4), see Sec. II C. In fact, the pressure field can be sampled randomly over an arbitrary volume, as shown in Sec. III.

B. Isotropy

A wave field is termed isotropic if the wavenumber vectors of the incident plane waves are uniformly distributed over all angles of incidence (corresponding to a sinusoidal distribution of the polar angles and a uniform distribution of the azimuth angles).[4] In order to evaluate isotropy in an acoustic field, it is necessary to analyze the direction of the waves that comprise the sound field. If the sound field is isotropic, its wavenumber spectrum is spherically symmetric (i.e., the magnitude of the waves is constant with angle). Contrarily, in an anisotropic sound field, the wavenumber

spectrum is asymmetric, as there is variable energy in different directions. Therefore, a spherical harmonic basis is best suited to analyze isotropy, as it depends only on the angles (polar and azimuth angles).

The magnitude of the wavenumber spectrum $\tilde{P}(\theta,\phi)$ determined in Eq. (6) is thus expanded into a series of spherical harmonics

$$|\tilde{P}(\theta,\phi)| = \sum_{n=0}^{\infty}\sum_{m=-n}^{n} A_{mn}(k_0)Y_n^m(\theta,\phi). \tag{7}$$

Since the spherical harmonics are orthonormal, the complex coefficients $A_{mn}(k_0)$ of the expansion can be calculated from

$$A_{mn}(k_0) = \int_0^{2\pi}\int_0^{\pi} |\tilde{P}(\theta,\phi)|Y_n^{m*}(\theta,\phi)\sin\theta d\theta d\phi. \tag{8}$$

It is interesting to note that Eq. (8) corresponds to a two-dimensional spherical Fourier transform.[31]

In the case of a perfectly isotropic sound field, the magnitude of the wavenumber spectrum is constant over the entire solid angle (i.e., spherically symmetric), which corresponds to a constant function over a sphere. Consequently, the energy of the wavenumber spectrum $\tilde{P}(\theta,\phi)$ resides entirely on the monopole moment of the spherical harmonic expansion in Eq. (7) [i.e., $A_{00}(k_0)$].[31] This will not be the case if the contributing waves cover just a partial section of the solid angle, as all moments of the spherical harmonic expansion in Eq. (7) would characterize the wave field (in the case of a single propagating plane wave, the magnitude of the wavenumber spectrum equals a Dirac delta function, the spherical Fourier coefficients of which are the spherical harmonics[31] $A_{mn} = [Y_n^m(\theta,\phi)]^*$). More generally, as soon as there is any degree of asymmetry in the wave field, part of the energy will be represented by the higher-order moments (which are spherically asymmetric).

The magnitude of the nth order moment is given by $\sum_{m=-n}^{n}|A_{mn}(k_0)|$, so that the relative magnitude of the monopole contribution (compared to the total orders) can now be expressed as

$$i(k_0) = \frac{|A_{00}(k_0)|}{\sum_{n=0}^{\infty}\sum_{m=-n}^{n}|A_{mn}(k_0)|}. \tag{9}$$

This quantity is here suggested as an isotropy indicator and will be denoted i in the following. The measure ranges between zero and one and equals unity in the case where the flow of acoustic energy is equal in all directions and is, therefore, perfectly isotropic. Conversely, it approaches zero if the incident waves propagate in a single direction. The measure is independent of the specific choice of coordinate directions. A similar measure was previously proposed in Ref. 32 for characterizing the radiation pattern of monopoles.

C. Implementation of the method

In practice, the two-dimensional wavenumber spectrum $\tilde{P}(\theta,\phi)$ is obtained using a discrete plane wave expansion, based on a discrete approximation of Eq. (4),

$$p(\mathbf{r}_m) = \sum_{l=1}^{L}\tilde{P}(\mathbf{k}_l)e^{-j\mathbf{k}_l\cdot\mathbf{r}_m}, \tag{10}$$

where the directions of propagation of the plane waves are uniformly distributed over a spherical domain. In the limit $L\to+\infty$ the pressure distribution in Eq. (4) is obtained.

The pressure field is sampled at a discrete number M of positions, and can be expressed in matrix form as

$$\mathbf{p} = \begin{bmatrix} \psi_1(\mathbf{r}_1) & \psi_2(\mathbf{r}_1) & \cdots & \psi_N(\mathbf{r}_1) \\ \vdots & \vdots & \ldots & \vdots \\ \psi_1(\mathbf{r}_M) & \psi_2(\mathbf{r}_M) & \cdots & \psi_N(\mathbf{r}_M) \end{bmatrix}\begin{bmatrix} c_1 \\ c_2 \\ \vdots \\ c_L \end{bmatrix}, \quad \mathbf{p} = \mathbf{W}\mathbf{c}, \tag{11}$$

where $\mathbf{p}$ is the measured sound pressure vector, $\mathbf{c}$ is a complex coefficient vector containing the wavenumber spectrum $\tilde{P}(\mathbf{k}_l)$ in Eq. (10) and $\mathbf{W}$ is a matrix containing the plane wave functions $\psi(\mathbf{r}) = e^{-j\mathbf{k}\cdot\mathbf{r}}$. This is an ill-posed (typically underdetermined) problem, which requires regularized inversion. The solution of Eq. (11) can be calculated in a least-squares sense, i.e., via a regularized matrix pseudo-inverse. The problem can be formulated as an unconstrained problem,[33] introducing a regularization parameter λ, which determines the penalty weight of the ℓ_p-norm of the solution vector. Throughout this study, the ℓ_2-norm of the solution is chosen,

$$\tilde{\mathbf{c}} = \underset{\mathbf{c}}{\operatorname{argmin}}(\|\mathbf{W}\mathbf{c}-\mathbf{p}\|_2^2 + \lambda\|\mathbf{c}\|_2^2), \tag{12}$$

which has the well-known closed form analytical solution

$$\tilde{\mathbf{c}} = \mathbf{W}^H(\mathbf{W}\mathbf{W}^H + \lambda\mathbf{I})^{-1}\mathbf{p}, \tag{13}$$

where the superscript H denotes the conjugate transpose and $\mathbf{I}$ is the identity matrix. Equation (13) corresponds to the least-squares solution of the problem with Tikhonov regularization.[34]

Subsequently, a spherical harmonic expansion of the magnitude of each component of $\mathbf{c}$ can be obtained based on a discrete approximation of Eqs. (7) and (8). Note however, that the discrete Fourier inversion required for calculating $\tilde{P}(\mathbf{k}_l)$ necessarily extends over a finite surface, limiting the angular resolution.

D. Numerical example

For the sake of illustration, we consider an *ideal* wavenumber spectrum [by *ideal*, we mean that the wavenumber spectrum $\tilde{P}(\theta,\phi)$ is estimated *perfectly*, hence disregarding numerical errors in the inversion of Eq. (11)], discretized into 1000 directions that are solutions to the so-called Thomson problem,[35] which considers equally charged particles on a sphere, hence yielding a uniform sampling over a spherical domain (Fig. 1). Two reference test cases are considered, where the sound field is modeled as (a) a single propagating plane wave; (b) a perfectly isotropic wave field. The complex coefficients A_{mn} from the spherical harmonic

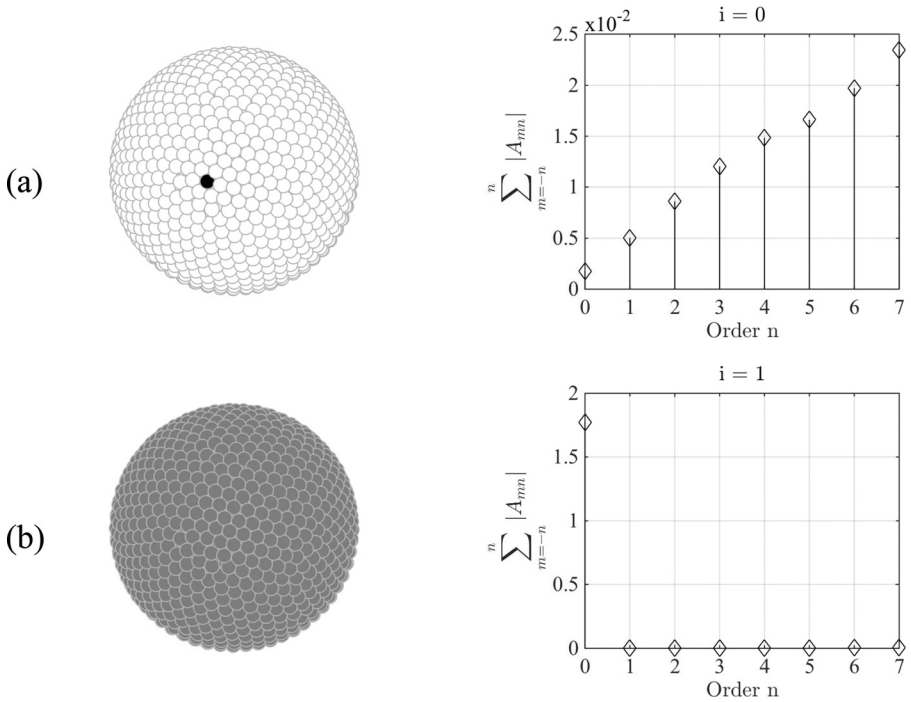

FIG. 1. Magnitude of the wavenumber spectrum and corresponding spherical harmonic expansion (up to $n=7$) in the ideal case of (a) a single propagating plane wave; (b) a perfectly isotropic sound field.

expansion in Eq. (7) are calculated using a discrete approximation of Eq. (8).

Figure 1 shows the magnitude of the *ideal* wavenumber spectra, along with the first seven moments (i.e., A_{mn} computed up to $n=7$) from their respective spherical harmonic expansions. The moments are displayed in terms of their magnitude $\sum_{m=-n}^{n}|A_{mn}|$. Figure 1(a) shows the case of the single propagating plane wave, which corresponds to a wavenumber spectrum with a single non-zero coefficient. It is apparent that all moments from the spherical harmonic expansion in Eq. (7) characterize the wave field and that the isotropy indicator in Eq. (9) is zero ($i=0$). Figure 1(b) displays the case of an ideal isotropic sound field, with a uniform spatial distribution of the directions of propagation of all waves. It can be seen that the wavenumber spectrum is rotationally symmetrical, and therefore its magnitude resides entirely on the monopole moment of the spherical harmonic expansion, i.e., all A_{mn} for $(m,\, n) \neq (0,0)$ are null. Analytically, the magnitude of such a spectrum corresponds to a constant function over the sphere. Consequently, the magnitude of the wavenumber spectrum is represented using the zeroth-order spherical harmonic only, and the indicator in Eq. (9) equals unity ($i=1$), indicating a perfectly isotropic sound field.

III. NUMERICAL RESULTS

A simulation is conducted to examine the validity of the method. The simulated pressure field is produced by a variable number of pure-tone point sources with equal volume velocity $Q=10^{-5}$ m^3s^{-1}. The resulting pressure field due to the monopoles is sampled at 64 randomly distributed points within a cubical volume of side length 20 cm, centred at the origin of coordinates (as shown in Fig. 2). The minimum distance between neighbouring measurement points is set to 5 cm.

All acoustic sources (monopoles) are distributed over a spherical domain of radius 2.4 m around the centre of the array. Thus, the complex pressures generated by the point sources are perfectly in phase at the array centre. Three different source configurations are simulated: seven sources evenly distributed over one-eighth of the spherical domain [case (a), see Fig. 3(a), left]; 26 sources evenly distributed over one-half of the spherical domain [case (b), see Fig. 3(b), left]; 52 sources evenly distributed over the entire spherical domain [case (c), see Fig. 3(c), left]. Additive noise of 30 dB signal-to-noise ratio is included in the simulated measurements.

For the plane-wave expansion described in Eq. (10), a plane-wave basis of 1000 plane waves of unknown amplitudes is considered, whose directions of propagation are distributed uniformly based on a Thomson problem.[35] The number of plane waves should be greater than the number of measurement positions, for a proper representation of the measured pressure.[26,36] The complex coefficient vector $\mathbf{c}$ corresponding to the wavenumber spectrum (i.e., the amplitudes of the waves) is estimated using Eq. (11). Tikhonov regularization [i.e., a ℓ_2 least-squares (LS) solution] is used

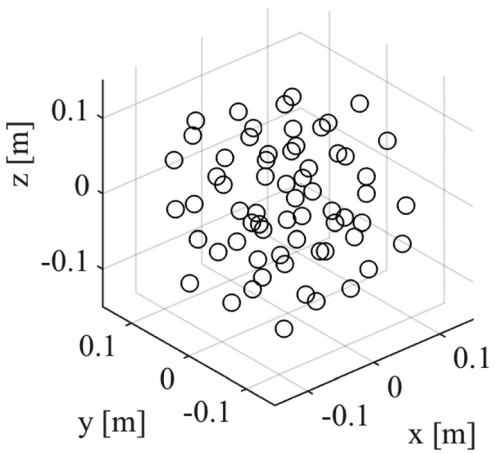

FIG. 2. Random spatial sampling of 64 positions.

for the regularized inversion, along with the L-curve criterion as a parameter-choice method.[34] As for the expansion of the wavenumber spectrum in Eq. (7), only a limited number of spherical harmonics orders can be used in practice. The spherical harmonic expansion is truncated at $n_{\text{trunc}} = N = 7$, corresponding to 64 coefficients [so that $(N+1)^2 = M$, where M is the number of measurement positions]. Although possible, adding more spherical harmonics in the expansion of the wavenumber spectrum does not contain relevant information.[37,38]

The resulting wavenumber spectra magnitudes $|P(\mathbf{k})|$ and corresponding spherical harmonic expansions are illustrated in Fig. 3 (centre and right columns, respectively) for the third-octave band centred at 500 Hz (the wavenumber results have been averaged over the third-octave band, and the spherical harmonic expansion conducted on the averaged wavenumber spectra). The moments from the respective spherical harmonic expansions are displayed in terms of their magnitude $\sum_{m=-n}^{n} |A_{mn}|$. In the first configuration [case (a), least isotropic configuration], the contributing waves cover a partial section of the solid angle, and therefore all moments are needed to describe the magnitude of the wavenumber spectrum. In the second scenario [case (b)], the contributing waves cover half of the solid angle, resulting in a wavenumber spectrum that is best described by the monopole and dipole moments of its spherical harmonic expansion. In the last case [case (c), most isotropic case], the wavenumber spectrum is nearly constant over the sphere, and therefore its magnitude resides primarily on the monopole moment of its spherical harmonic expansion, i.e., A_{mn} for $(m, n) \neq (0, 0)$ are (almost) null. These results are well in line with the estimated isotropy indicator values: 0.17, 0.38, and 0.96, for the three cases, respectively.

Figure 4 shows the isotropy indicators of cases (a), (b), and (c) as a function of frequency, for the third-octave bands ranging from 125 Hz to 1 kHz. The results confirm the isotropy of sound field (c) in the entire frequency range (values ranging between 0.93 and 0.97). The indicator is not unity because the sound field is due to 52 sources only (and therefore not perfectly isotropic).

The robustness to noise of the method is examined in Appendix B.

IV. EXPERIMENTAL RESULTS

The validity of the proposed methodology is examined experimentally in a large (215 m^3) reverberation room at the Technical University of Denmark (DTU), with two different

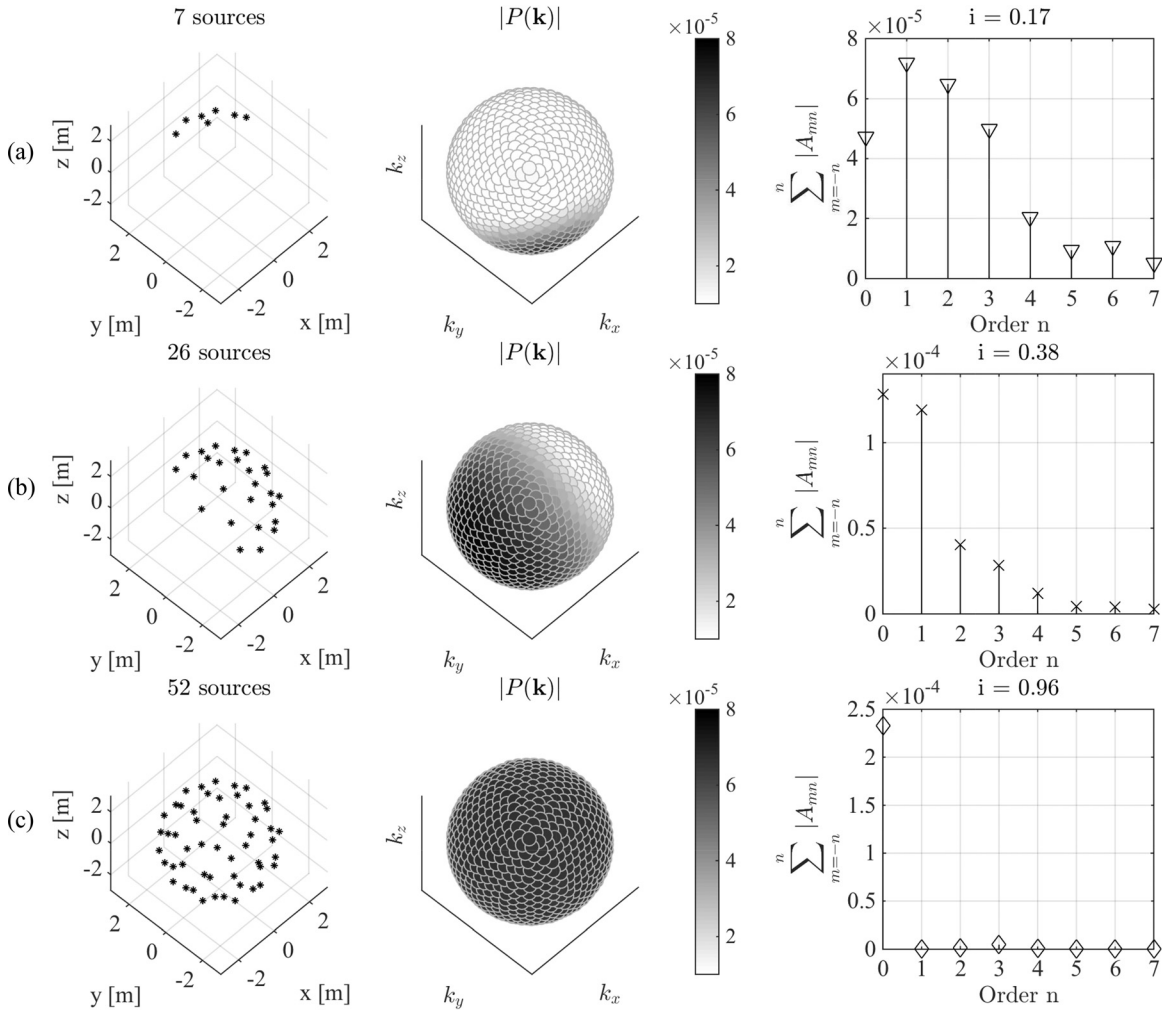

FIG. 3. Monopoles distribution, wavenumber spectrum and corresponding spherical harmonic expansion for sound fields (a), (b), and (c), respectively (top to bottom). Frequency: 500 Hz. Truncation order: $N = 7$.

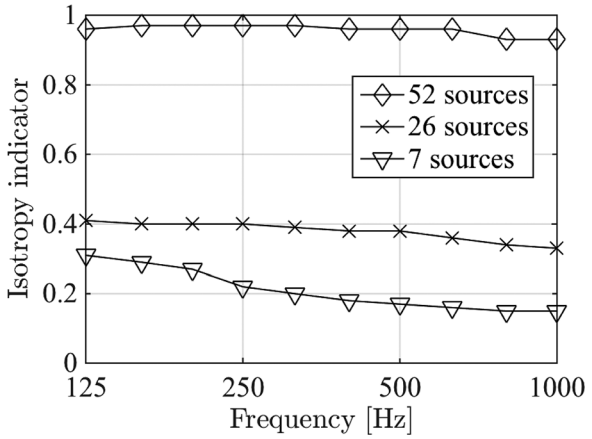

FIG. 4. Isotropy indicator as a function of frequency for the sound fields (a), (b), and (c). Truncation order: $N = 7$.

damping conditions. Validation measurements are also conducted in the DTU anechoic chamber (1000 m^3) and in the DTU Audio Visual Immersion Lab (AVIL), for they provide tractable environments to examine the methodology. All measurements are performed using a rigid spherical microphone array of radius $a = 9.75$ cm (Brüel & Kjær, Nærum, Denmark, see Fig. 5). The array consists of 64 microphones near-uniformly distributed over its surface, and can sample up to 7 orders of spherical harmonics.

Spherical microphone arrays are widely used for the analysis and reconstruction of complex sound fields[33,39] and are particularly well suited for applications in enclosures,[40] where the sound waves impinge on the array from multiple directions. Hence, several authors have proposed methods for quantifying diffuseness or isotropy, using spherical array measurements.[17,18,23,24] The approach described in this work does not require a specific array configuration. We use the spherical array here (unlike in Sec. III) for convenience, as this equipment is readily available. Note that the scattering induced by the presence of the rigid sphere in the medium is accounted and compensated for.[33]

As in Sec. III, a plane-wave basis of 1000 plane waves is considered for the plane-wave expansion described in Eq. (10), and the spherical harmonic expansion of the wavenumber spectrum is truncated at $n_{\text{trunc}} = N = 7$.

FIG. 5. Sixty-four-channels rigid spherical microphone array.

A. Experimental results in the anechoic chamber

An omnidirectional source (an "Omnisource," Brüel & Kjær), which radiates approximately like a point source, is placed 4 m away from the surface of the rigid spherical array. The source is driven with random white noise, and a spectral resolution of 1 Hz is used for the analysis. The pressure on the surface of the array is shown in Fig. 6(a) at 500 Hz ($ka = 0.89$). Tikhonov regularization is used for the regularized inversion of Eq. (11), along with the L-curve

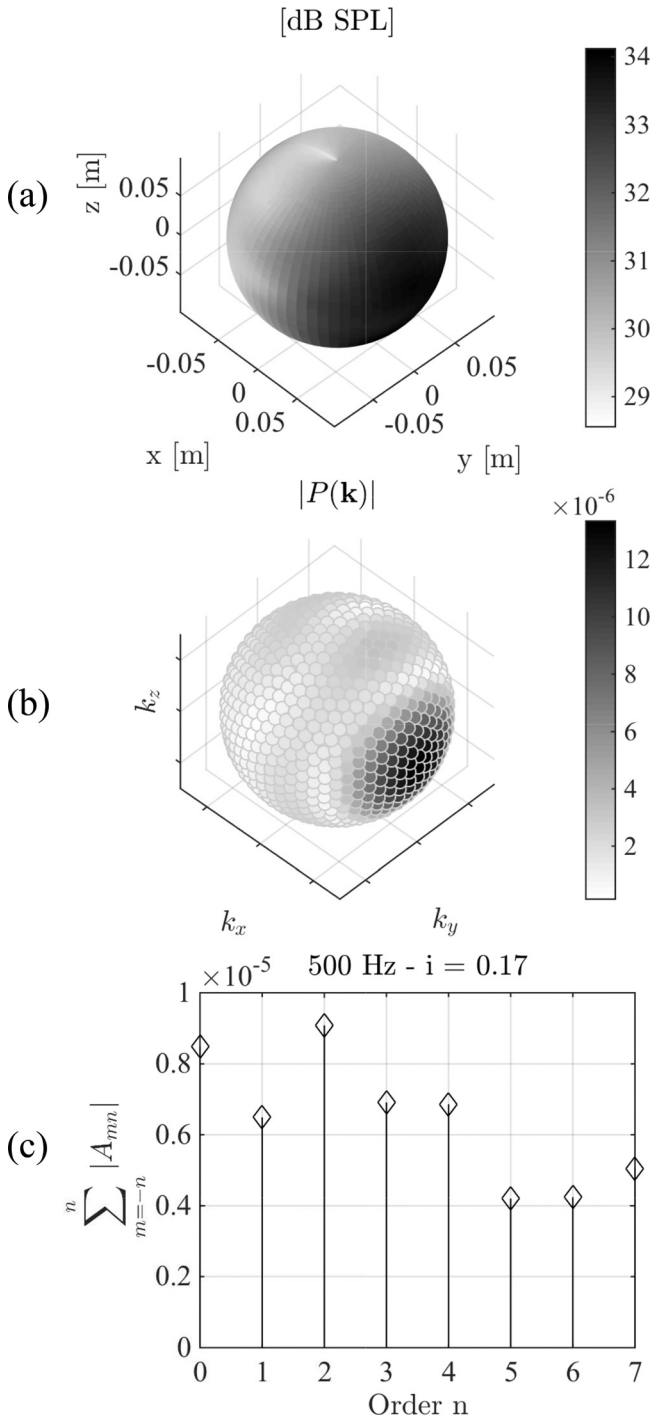

FIG. 6. Sound pressure level measured in the anechoic chamber at the 64 microphone positions (a); wavenumber spectrum, rotated for display convenience (b); spherical harmonic expansion (c). Frequency: 500 Hz. Truncation order: $N = 7$.

criterion as a parameter-choice method,[34] to estimate the wavenumber spectrum.

Figures 6(b) and 6(c), respectively, show the wavenumber spectrum magnitude, and corresponding spherical harmonic expansion for the third-octave band centred at 500 Hz. It is apparent that all moments from the spherical expansion in Eq. (7) are needed to describe the magnitude of the angular spectrum, which in turn confirms the anisotropy of the sound field. Nevertheless, the angular resolution of the estimated wavenumber spectrum is compromised (the response exhibits a main lobe and concentric side lobes, as in a conventional array output)[41] due to the limited measurement aperture. Hence, the isotropy indicator resulting from the least-squares solution is likely to have higher values than expected throughout the whole frequency range. In the present case of a single wave impinging on the array, the use of the compressive sensing (CS) framework would significantly improve the angular resolution,[42] leading to a wavenumber spectrum closer to that in Fig. 1(a). This is shown in Appendix A. However, in this study, the conventional least-squares solution with Tikhonov regularization is chosen instead, as this choice is more appropriate for rooms and enclosures, where the wave field cannot be assumed to be spatially sparse.

Figure 7 shows the estimated isotropy indicator as a function of frequency for the third-octave bands ranging from 125 Hz to 1 kHz. The corresponding wavenumber spectra are also shown. At low frequencies, the spatial resolution is poor (as the wavelength is large compared to the dimension of the array, $ka < 0.45$), leading to a wide main lobe in the wavenumber spectrum. This in turn results in an isotropy indicator ranging between 0.25 and 0.35. At medium frequencies ($0.45 < ka < 0.89$), the resolution of the array is finer and the isotropy indicator has values around 0.2. At high frequencies ($ka > 0.89$), the resolution is higher (the main lobe and side lobes are therefore narrower), leading to an isotropy indicator below 0.2. Ideally, the isotropy indicator would be zero, as shown in Sec. II D, but it is not zero because of the regularization employed. When using a sparse regularization approach (see Appendix A), the indicator drops to 0.02 in the entire frequency range.

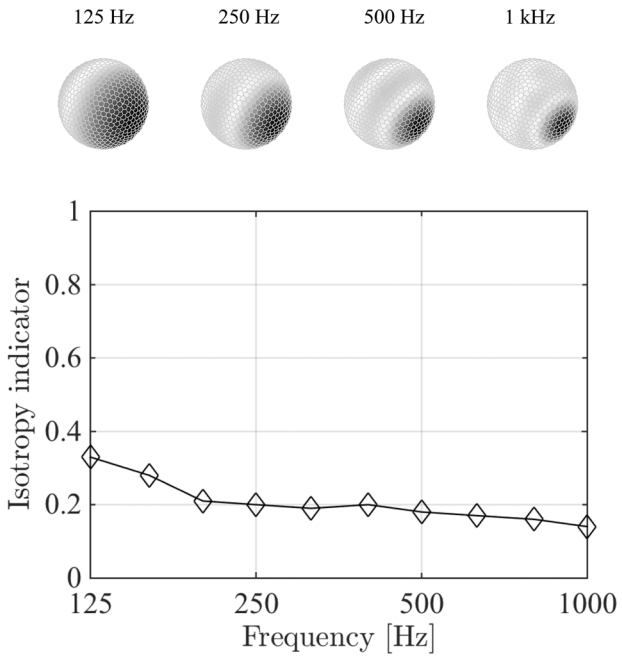

FIG. 7. Isotropy indicator as a function of frequency in the anechoic chamber (bottom, truncation order: $N = 7$) and corresponding wavenumber spectra at 125 Hz, 250 Hz, 500 Hz, and 1 kHz (top).

B. Experimental results in a sound field reproduction room

An experimental test is conducted using a 64-channel loudspeaker array, set in an anechoic chamber (Audio Visual Immersion Lab, AVIL, at DTU). The 64 loudspeakers (KEF LS50) are arranged over a spherical domain of radius 2.4 m, thereby surrounding the rigid spherical microphone array (i.e., the microphone array is placed at the centre of the loudspeaker array, so that the distance between any of the loudspeakers and the centre of the microphone array is 2.4 m, see Fig. 8). Only 52 out of the 64 available speakers were used for the experiment, so as to obtain a (quasi) uniform distribution of sources over the spherical domain. It should be noted that the speakers are not only positioned above and around the array, but also below the laboratory's suspended floor.

The speakers, which radiate approximately like point sources, are driven with random white noise signals with equal power, so as to approximate a homogeneous and isotropic sound field. Since the sources are uncorrelated, this experimental arrangement corresponds to an approximation to the perfect diffuse sound field as described in Ref. 4 and in the experimental investigation of Ref. 14. The pressure at the 64 microphone positions is calculated based on the measured autospectra. Although this is sufficient for the purpose of this study, one cannot possibly disregard the phase of the pressure signals when evaluating sound field diffusion in a room.[18,43]

Figure 9 shows the pressure on the surface of the array at 125 Hz [Fig. 9(a)] and 400 Hz [Fig. 9(b)], the resulting wavenumber spectra (averaged over the respective third-octave bands of frequencies) and the corresponding spherical harmonic expansions ($N = 7$). As in Sec. IV A, Tikhonov regularization is used for the regularized inversion, along

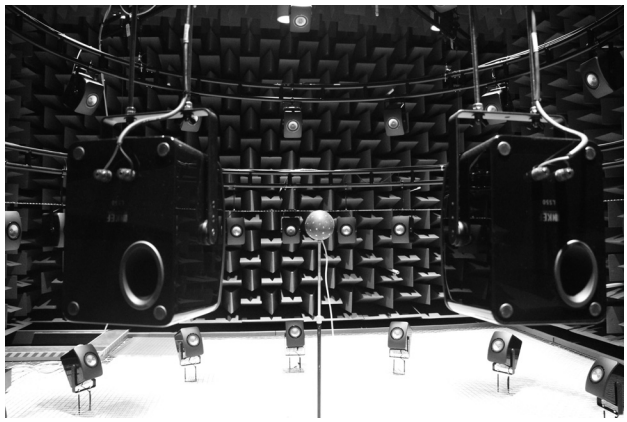

FIG. 8. Sixty-four-channel loudspeaker array (Audio Visual Immersion Lab, AVIL, DTU).

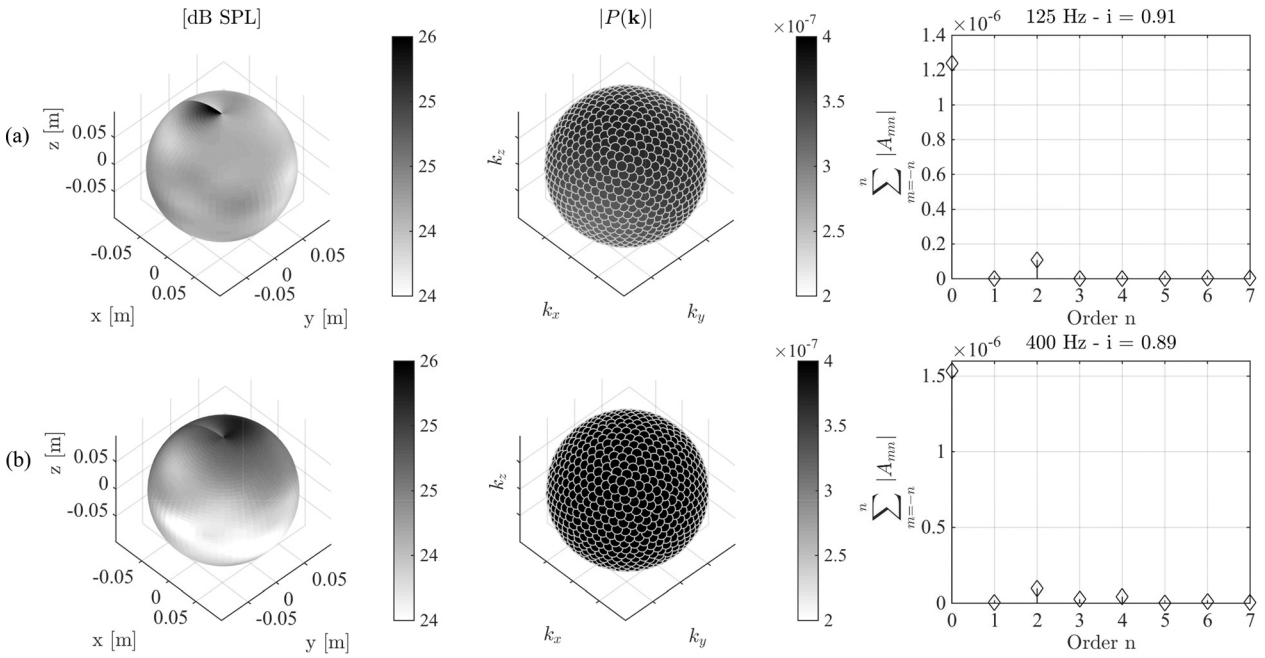

FIG. 9. Measured pressure, wavenumber spectrum and spherical harmonic expansion at 125 Hz (a) and 400 Hz (b), due to a set of 52 loudspeakers emitting random white noise of equal power. Truncation order: $N = 7$.

with the L-curve criterion as a parameter-choice method. In both cases, the measured pressure has variations of ± 1 dB, resulting in a wavenumber spectrum that is nearly constant over the spherical domain. Therefore, its magnitude is best described by the zeroth-order moment of its spherical harmonic expansion. At 125 Hz the isotropy indicator is 0.91, and 0.89 at 400 Hz. It does not reach exactly unity, due to errors resulting from differences in the speakers' frequency responses (± 2 dB), positioning errors, and transducer mismatch.

C. Experimental results in the reverberation room

Experiments are conducted in a large (215 m^3) reverberation room, both empty and with an added sample of absorptive material on the floor. Figure 10(a) shows the absorption coefficient of the 10.8 m^2 sample, measured according to ISO 354 (Ref. 1) in one-third octave bands using the interrupted noise method and a Brüel & Kjær sound level meter (type 2250). The room complies with the ISO 354 requirements,[1] and is essentially rectangular although there are 85 built-in concrete boundary diffusers and 12 hanging panel diffusers [see Fig. 10(b)]. The room is driven to steady-state conditions with random white noise using a built-in loudspeaker placed in one of the upper-corners of the room (that is, at a sufficiently large distance away from the surface of the rigid spherical array, so as to maximally excite the room modes and reduce the amount of direct radiation on the surface of the array). A spectral resolution of 0.125 Hz is used for the analysis, corresponding to a time window of 8 s. This corresponds to measuring at 6400 independent discrete frequencies with a frequency span of 800 Hz. The measurements cover the third-octave bands ranging from 125 Hz to 1 kHz. Once again, Tikhonov regularization is used for the regularized inversion, along with the L-curve criterion as a parameter-choice method.

Figures 11(a) and 11(b) compare the resulting wavenumber spectrum at 1 kHz, in the empty and damped room. In the undamped room [free of absorption, Fig. 11(a)], a few dominant incident directions are detected (i.e., a few waves that carry considerably more energy than others, seemingly

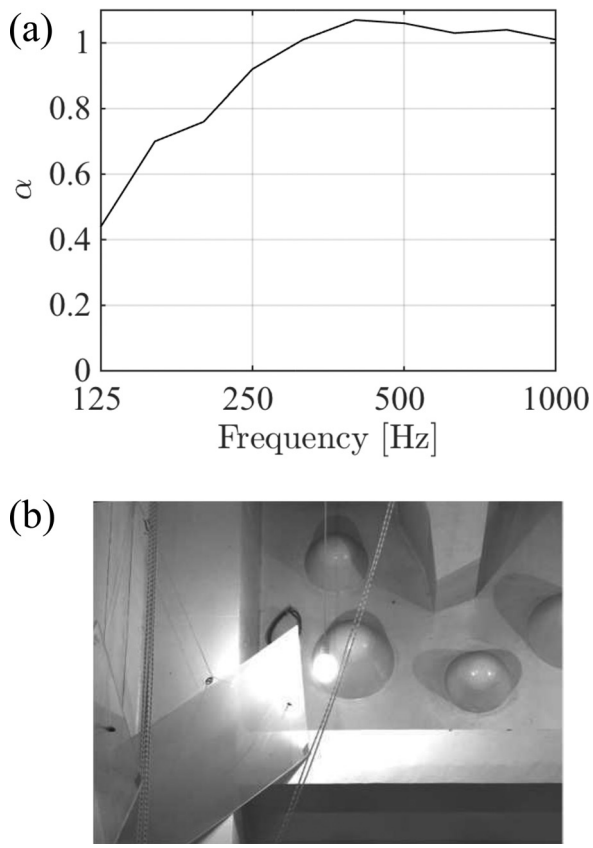

FIG. 10. Absorption coefficient of the specimen as a function of frequency (a); panel and boundary diffusers in the test room (b).

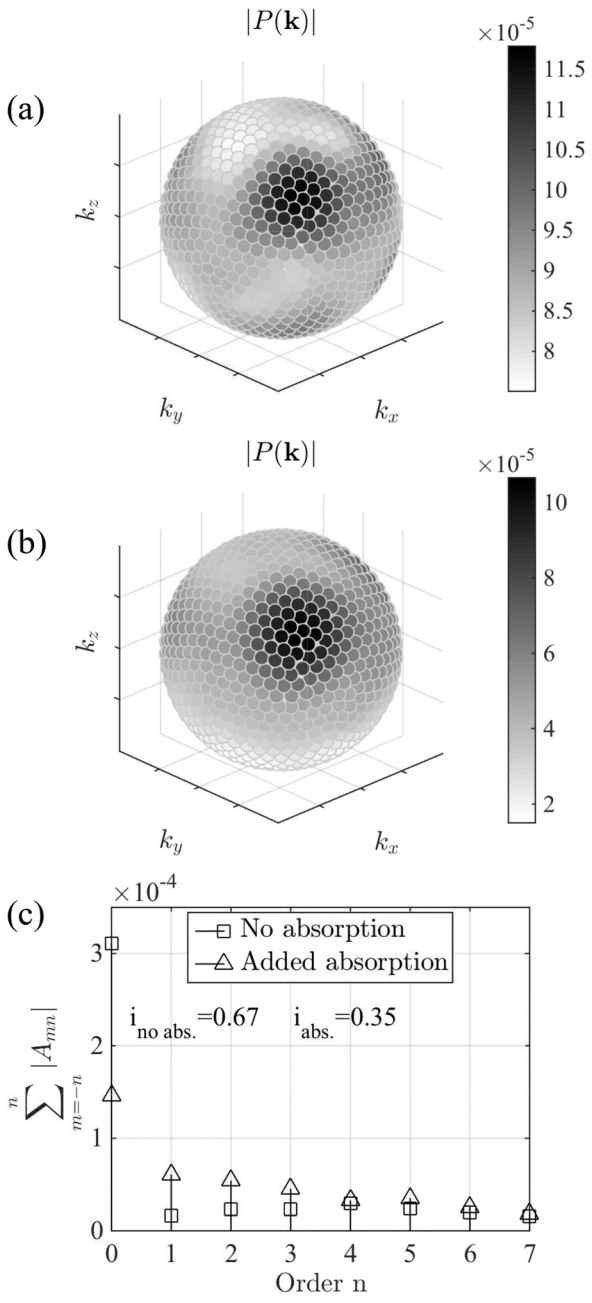

FIG. 11. Magnitude of the wavenumber spectrum (rotated for display convenience) in the empty reverberation room (a) and in the room with added absorption (b); corresponding spherical harmonic expansions (c). Frequency: 1 kHz. Truncation order: $N = 7$.

corresponding to the direct radiation from the source and a few early reflections), indicating that the field is not perfectly isotropic [as would be the case in the ideal example shown in Fig. 1(b)]. In the damped room [added absorption, Fig. 11(b)], the wavenumber spectrum is less omnidirectional, as there are no waves propagating in the positive z-direction, because no sound is being reflected by the absorbing sample ($\alpha \approx 1$ at 1 kHz). This is in good agreement with results described in Ref. 40, which show that there exists a large influx of energy directed towards the absorber. The results are confirmed by the corresponding spherical harmonic expansions displayed in Fig. 11(c) ($N = 7$). In the undamped case, the wavenumber spectrum is best described by the

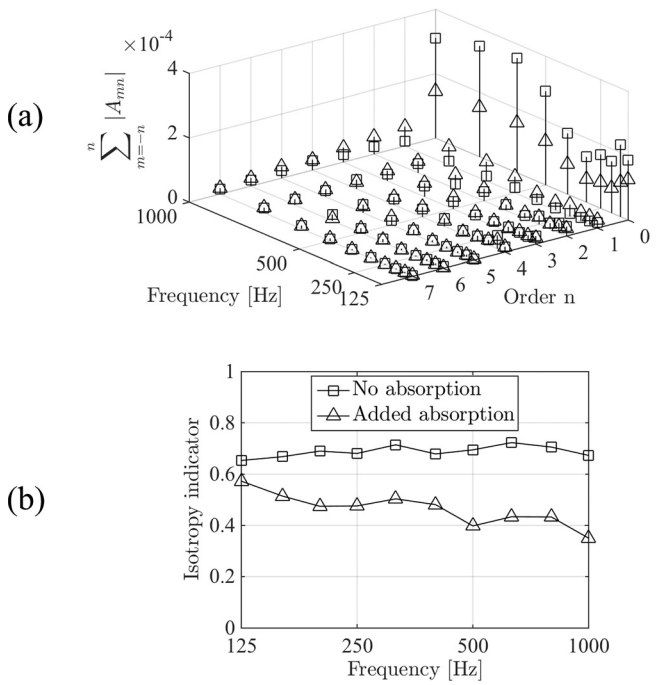

FIG. 12. Spherical harmonic expansions as a function of frequency in the empty and damped reverberation rooms (a); Corresponding isotropy indicator as a function of frequency (b). Truncation order: $N = 7$.

monopole moment of its spherical harmonic expansion, yielding an isotropy indicator value of $i = 0.67$. The sound field is not perfectly isotropic, due to the few dominant directions in the wavenumber spectrum (the stationary sound field in a reverberation chamber driven with a single source is, in fact, not expected to be fully isotropic). In the damped case, the spherical harmonic expansion is no longer dominated by the monopole moment, resulting in a sound field that is less isotropic than in the empty room ($i = 0.35$).

Figure 12(a) compares the magnitude of the moments from the spherical harmonic expansions in the undamped and damped room, for the third-octave bands ranging from 125 Hz to 1 kHz. Figure 12(b) shows the corresponding isotropy indicators as a function of frequency. In the undamped room, the monopole moment dominates the spherical harmonic expansion of the wavenumber spectrum throughout the entire frequency range, yielding values of the isotropy indicator that range from 0.65 to 0.72. In the damped room, higher-order moments are required to describe the wavenumber spectrum. The isotropy indicator in this case ranges from 0.35 to 0.57, indicating that the sound field is less isotropic than in the undamped case. At low frequencies (below 400 Hz), the isotropy indicator is greater than at high frequencies, because the absorption in the room is lower. In fact, it can be observed that the absorption of the material [see Fig. 10(a)] influences the isotropy of the sound field: as the absorption increases, isotropy tends to decrease.

V. DISCUSSION

The current measurement system (64-channels microphone array of radius 9.75 cm) is not expected to provide valid results below 120 Hz, where the circumference of the

sphere corresponds to about 10% of the wavelength in air ($ka = 0.1$), nor at high frequencies, where aliasing effects start to appear. In the operational frequency range of the array, the results indicate that the isotropy indicator responds correctly to changes in the isotropy of the sound field. The robustness to noise of the method is examined in Appendix B, which shows that the method is fairly robust to perturbations for SNRs as low as 20 dB, a common range in room acoustic measurements. Nevertheless, its accuracy depends on the wavenumber spectrum estimation, which relies on (a) the measurement system: the sampling of the pressure field should be sufficient to estimate its wavenumber spectrum correctly; (b) the choice of the regularization scheme: in the present study, the wavenumber spectrum has been calculated via a conventional regularized least-squares inversion. This is a sensible choice for estimating the wave field in a reverberant room. However, alternative solution strategies (ℓ_1-norm, elastic-net, etc.) can be further examined.[42,44] An alternate estimation of the wavenumber spectrum based on the framework provided by CS is presented in Appendix A, with application to sparse problems.

An advantage of the approach described in this work is that it does not require a specific array configuration. As briefly mentioned in the introduction, other methods have been proposed for the estimation of diffuseness from a set of measured microphone signals. Epain and Jin[18] suggested characterizing diffuseness based on the analysis of the spherical harmonic covariance matrix. Yet, the analysis in the spherical harmonic domain is performed on the recorded signals directly (rather than on the wavenumber spectrum), requiring the use of a spherical array of microphones. Moreover, the study is concerned with the estimation of diffuseness arising from the presence of multiple sources. The sound field in a reverberation room driven with noise from one source is, of course, quite different.

This work examines steady-state sound fields in a reverberation chamber. The results evaluate how isotropic the sound field is at a particular location of the room; hence, they do not directly evaluate the compliance of the reverberation room with ISO 354:2003 and ISO 140–10:1991 (which assume the sound field to be perfectly isotropic[1,2]). For this purpose, extended measurements should be conducted.

The analytical framework considers the sound field produced by a pure-tone in a reverberant enclosure. However, we eventually average the wavenumber spectrum results over a third-octave band of frequencies. These results are correct on average since the frequency components of the experimental random noise have random phases.

VI. CONCLUSION

An experimental method to evaluate sound field isotropy in enclosures is proposed in this study. The method is based on an analysis of the wavenumber spectrum in the spherical harmonics domain, which has suitable mathematical properties when it comes to examine isotropy.

Since the spherical harmonic expansion is performed on the wavenumber spectrum, and contrary to existing methods, the proposed method is not restricted to measurements with a spherical array, and the pressure field can be sampled arbitrarily (e.g., using regular or random spatial sampling schemes). Furthermore, because of being formulated as an elementary wave model, the wavenumber spectrum can be obtained in a least-square sense using conventional regularization schemes, but also allows for alternative strategies (ℓ_1-norm, elastic-net, etc.), conferring a broader application perspective.

The numerical and experimental results obtained in two anechoic chambers (one with a single source and another with an array of 52 sources uniformly distributed around a spherical microphone array) and in a reverberation chamber (both empty and with absorption on the floor) indicate that the method is suitable for assessing the isotropy of a sound field. The results convey an interesting prospect for characterizing the diffuse field conditions in enclosures.

ACKNOWLEDGMENTS

The authors would like to thank Antoine Richard and Marton Marschall for help with the experimental arrangement, and John L. Davy for comments and discussion. This work is funded by the Oticon Foundation.

APPENDIX A: WAVENUMBER ESTIMATION FOR SPARSE PROBLEMS

In the case of few sound waves impinging on the array, solving the system of linear equations in Eq. (11) via ℓ_2-minimization yields a poor representation of the measured data (i.e., the solution tends to produce many non-zero coefficients), compromising the angular resolution, and consequently the value of the isotropy indicator. An alternate estimation of the wavenumber is based on the framework provided by CS that promotes a sparse solution to the problem (i.e., an optimal representation of the measured data with as few non-zero coefficients as possible) via ℓ_1-minimization.[42] The problem can be formulated in an unconstrained form by introducing a regularization parameter λ which determines the weight of the ℓ_1-norm penalty:

$$\tilde{\mathbf{c}} = \underset{\mathbf{c}}{\operatorname{argmin}} \|\mathbf{W}\mathbf{c} - \mathbf{p}\|_2^2 + \lambda\|\mathbf{c}\|_1. \tag{A1}$$

Equation (A1), which corresponds to the well-known LASSO formulation,[45] is identical to Eq. (12), but using the ℓ_1-norm $\|\cdot\|_1$ instead.

The method is examined experimentally, based on the anechoic measurements introduced in Sec. IV A. The ℓ_2 least-squares (LS) solution obtained with Tikhonov regularization is compared with the CS (LASSO) solution. The CS solution is obtained as in Eq. (A1), and the LS solution is calculated as in Eq. (12).

Figure 13(a) shows the magnitude of the wavenumber spectrum resulting from the LS [Eq. (12)] and the CS [Eq. (A1)] solutions, respectively, for the third-octave band centred at 500 Hz. It is apparent that the obtained complex coefficients are significantly different. In the LS approach all of the wavenumber coefficients are non-zero, whereas the CS solution returns approximately four non-zero coefficients,

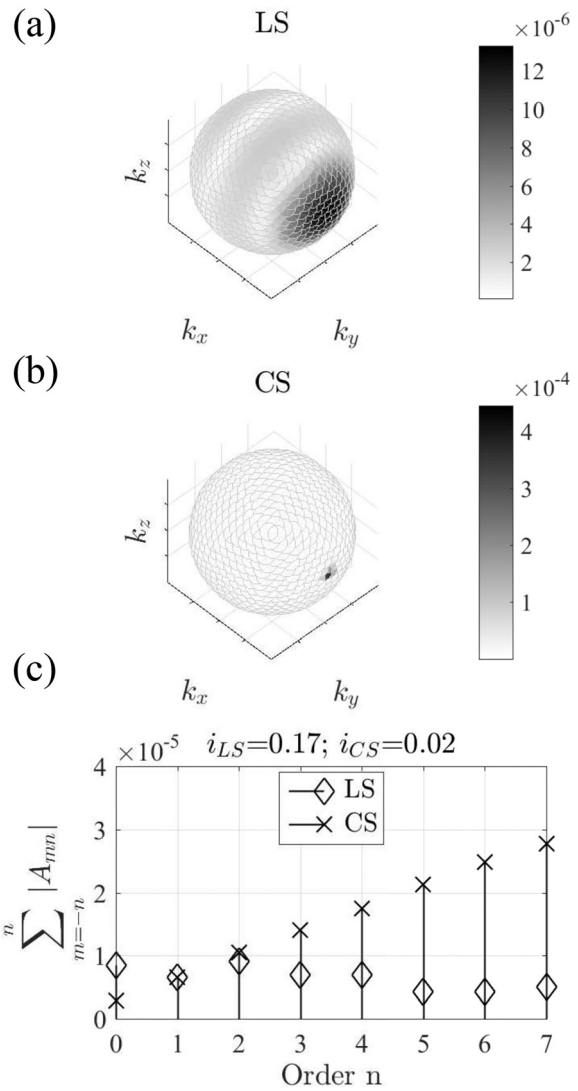

FIG. 13. Magnitude of the wavenumber spectrum in the anechoic chamber resulting from the LS (top) and CS (middle) solutions, respectively (a); corresponding spherical harmonic expansions (b). Frequency: 500 Hz. Truncation order: $N = 7$.

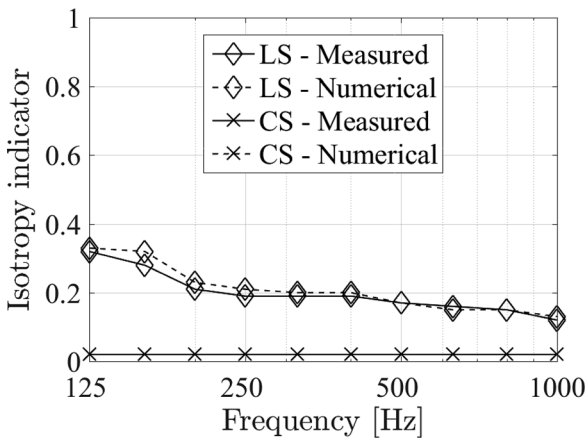

FIG. 14. Isotropy indicator resulting from the LS and CS solutions, respectively, as a function of frequency in the anechoic chamber. Numerical predictions are superimposed. Truncation order: $N = 7$.

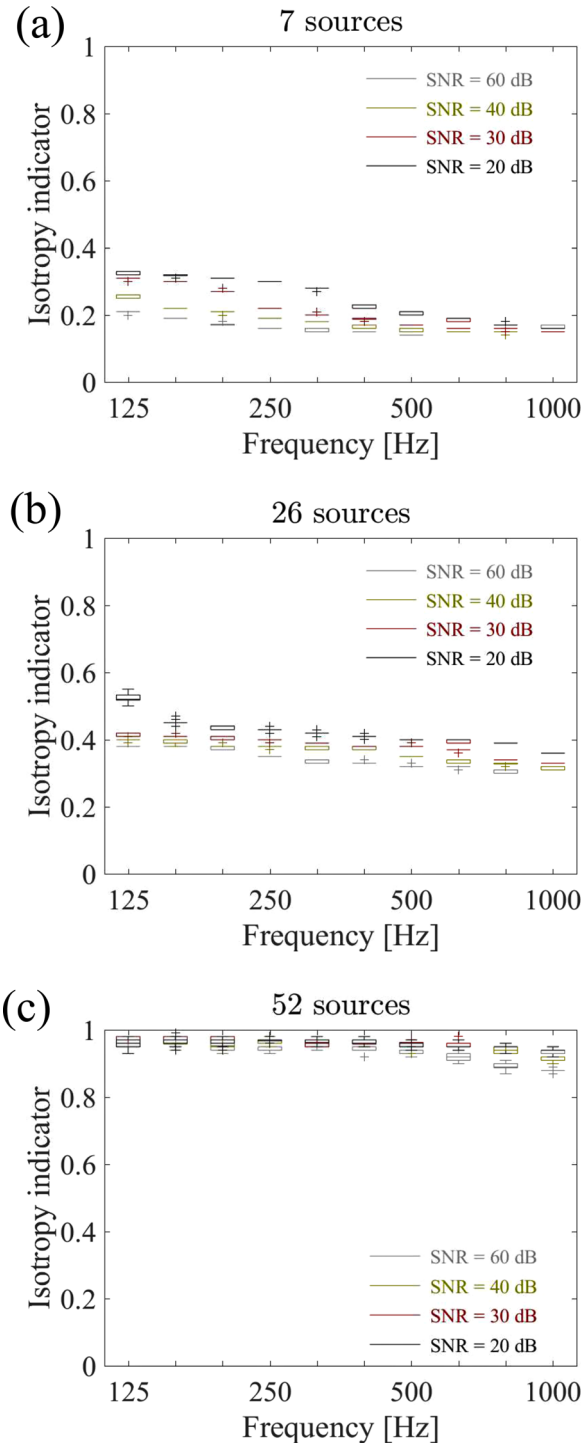

FIG. 15. (Color online) Box plots of the isotropy indicator as a function of frequency, for the numerical study presented in Sec. III. The SNR values vary between 20 dB SNR and 60 dB SNR. Truncation order: $N = 7$.

yielding a wavenumber spectrum that resembles roughly a Dirac delta function on the sphere. This in turn indicates that the CS solution accurately detects the incoming direction of the waves used in the expansion in Eq. (10) (i.e., the direction of arrival of the waves radiated by the loudspeaker). Figure 13(b) compares the corresponding spherical harmonic expansions of the wavenumber spectra resulting from the LS and CS estimations, respectively ($N = 7$). The CS solution results in less energy in the monopole moment and lower order moments, in good agreement with the results obtained

in the ideal case of a single propagating wave, as illustrated in Fig. 1(a). The LS solution yields an isotropy indicator value of 0.17, whereas the CS solution results in a value of 0.02, much closer to zero, representing accurately the anisotropy of the sound field.

Figure 14 shows the isotropy indicator as a function of frequency, for the third-octave bands ranging from 125 Hz to 1 kHz, resulting from the LS and CS [Eq. (A1)] solutions, respectively. It is apparent that the LS solution overestimates the isotropy indicator, whereas the CS solution yields values close to zero throughout the entire frequency range, in agreement with the theoretical considerations presented in Sec. II. Nonetheless, selecting the ℓ_1-norm is a poor regularization choice when processing the sound field in reverberant enclosures, which yields non-physical solutions since the problem is not sparse. A ℓ_2 least-squares solution with Tikhonov regularization is therefore best suited to applications in rooms. Further numerical results were determined based on simulated measurements using an identical 9.75 cm radius rigid-sphere array with 64 microphones. The predicted isotropy indicators resulting from the LS and CS solutions, respectively, are superimposed to the experimental values. There is fair, if not perfect, agreement between predictions and experimental results.

APPENDIX B: ROBUSTNESS TO NOISE

The influence of the signal-to-noise ratio (SNR) on the evaluation of the isotropy indicator is investigated, based on the numerical study presented in Sec. III. Figure 15 shows box plots of the isotropy indicator as a function of frequency, for the same source configurations as in Sec. III [Figs. 15(a), 15(b), and 15(c), respectively] and SNR values varying between 20 dB SNR and 60 dB SNR. For each SNR, the isotropy indicators have been computed for 25 separate realizations, over the third-octave bands ranging from 125 Hz to 1 kHz. The central marks in the figures are the median of the isotropy indicator, the box represents the first and third quartiles (isotropy indicator between 25% and 75%), and the whiskers are 1.5 times the interquartile distance. Outliers outside this range are removed and correspond to wrong automatic-choice regularization parameters that can be detected from inspection of the L-curve. For the three test cases, the results show that the method is robust to perturbations up to 20 dB SNR, which is sufficient, as noise levels in room acoustic measurements are typically lower.

[1]ISO 354:2003, "Measurement of sound absorption in a reverberation room" (International Organization for Standardization, Geneva, Switzerland, 2003).
[2]ISO 140-10:1991, "Acoustic—Measurement of sound insulation in buildings and of building elements. Part 10: Laboratory measurement of airborne sound insulation of small building elements" (International Organization for Standardization, Geneva, Switzerland, 1991).
[3]T. J. Schultz, "Diffusion in reverberation rooms," J. Sound Vib. **16**, 17–28 (1971).
[4]F. Jacobsen, "The diffuse sound field," Ph.D. thesis, The Acoustics Laboratory, Technical University of Denmark, Kongens Lyngby, Denmark, 1979.
[5]R. H. Lyon, "Needed: A new definition of diffusion," J. Acoust. Soc. Am. **56**, 1300–1302 (1974).
[6]J.-D. Polack, "Modifying chambers to play billiards–The foundation of reverberation theory," Acustica **76**(6), 257–272 (1992).
[7]M. R. Schroeder, "Statistical parameters of the frequency response curves of large rooms," J. Audio Eng. Soc. **35**(5), 299–306 (1987); originally published in German in Acustica **4**, 594–600 (1954).
[8]R. V. Waterhouse, "Statistical properties of reverberant sound fields," J. Acoust. Soc. Am. **43**, 1436–1444 (1968).
[9]D. Lubman, "Fluctuations of sound with position in a reverberant room," J. Acoust. Soc. Am. **44**, 1491–1502 (1968).
[10]F. Jacobsen, "Active and reactive sound intensity in a reverberant sound field," J. Sound Vib. **143**, 231–240 (1990).
[11]F. Jacobsen and A. Rodríguez Molares, "The ensemble variance of pure-tone measurements in reverberation rooms" J. Acoust. Soc. Am. **127**, 233–237 (2010).
[12]A. D. Pierce, *Acoustics: An Introduction to Its Physical Principles and Applications* (McGraw-Hill, New York, 1981), Secs. 6.3 and 6.1.
[13]R. K. Cook, R. V. Waterhouse, R. D. Berendt, S. Edelman, and M. C. Thompson, Jr., "Measurement of correlation coefficients in reverberant sound fields," J. Acoust. Soc. Am. **27**, 1072–1077 (1955).
[14]K. Bodlund, "A new quantity for comparative measurements concerning the diffusion of stationary fields," J. Sound Vib. **44**(2), 191–207 (1976).
[15]F. Jacobsen and T. Roisin, "The coherence of reverberant sound fields," J. Acoust. Soc. Am. **108**, 204–210 (2000).
[16]K. J. Ebeling, "Statistical properties of random wave fields," in *Physical Acoustics, Principles and Methods*, edited by W. P. Mason and R. N. Thurston (Academic, New York, 1984), Vol. XVII, Chap. 4, Secs. 3 and 4, pp. 246–265.
[17]B. N. Gover, J. Ryan, and M. Stinson, "Measurements of directional properties of reverberant sound fields in rooms using a spherical microphone array," J. Acoust. Soc. Am. **116**(4), 2138–2148 (2004).
[18]N. Epain and C. T. Jin, "Spherical harmonic signal covariance and sound field diffuseness," IEEE/ACM Trans. Audio, Speech, Lang. Process. **10**(24), 1796–1807 (2016).
[19]C.-H. Jeong, F. Jacobsen, and J. Brunskog, "Thresholds for the slope ratio in determining transition time and quantifying diffuser performance *in situ*," J. Acoust. Soc. Am. **132**, 1427–1435 (2012).
[20]R. Prislan, J. Brunskog, F. Jacobsen, and C.-H. Jeong, "An objective measure for the sensitivity of room impulse response and its link to a diffuse sound field," J. Acoust. Soc. Am. **136**(4), 1654–1665 (2014).
[21]T. Hanyu and K. Hoshi, "Evaluation of isotropy of sound field in a room based on the decay-cancelled sound intensity," in *Proceedings of the 22nd International Congress on Acoustics*, Buenos Aires, Argentina (2016).
[22]C.-H. Jeong, "Kurtosis of room impulse responses as a diffuseness measure for reverberation chambers," J. Acoust. Soc. Am. **139**(5), 2833–2841 (2016).
[23]V. Pulkki, A. Politis, M.–V. Laitinen, J. Vilkamo, and J. Ahonen, "First-order directional audio coding (DirAC)," in *Parametric Time-Frequency Domain Spatial Audio* (Wiley, New York, 2017), Chap. 5, pp. 89–138.
[24]P. Götz, K. Kowalczyk, A. Silzle, and E. A. P. Habets, "Mixing time prediction using spherical microphone arrays," J. Acoust. Soc. Am. **137**(2), EL206–EL212 (2015).
[25]ISO 3741-1999, "Acoustics—Determination of sound power levels of noise sources using sound pressure—Precision methods for reverberation rooms" (International Organization for Standardization, Geneva, Switzerland, 1999).
[26]E. G. Williams, *Fourier Acoustics: Sound Radiation and Near-Field Acoustical Holography* (Academic, New York, 1999).
[27]P. Baldi and D. Marinucci, "Some characterizations of the spherical harmonics coefficients for isotropic random fields," Stat. Probab. Lett. **77**, 490–496 (2007).
[28]S. Kumar, A. Rotti, M. Aich, N. Pant, S. Mitra, and T. Souradeep, "Orthogonal bipolar spherical harmonics measures: Scrutinizing sources of isotropy violation," Phys. Rev. D **91**, 043501 (2015).
[29]J. A. S. Angus, "Diffuser assessment using surface spherical harmonics," J. Acoust. Soc. Am. **104**, 1857 (1998).
[30]M. Müller-Trapet, M. Pollow, and M. Vorländer, "Spherical harmonics as a basis for quantifying scattering and diffusing objects," in *Proceedings of Forum Acusticum 2011*, Aalborg, Denmark (2011).
[31]B. Rafaely, *Fundamentals of Spherical Array Processing* (Springer-Verlag, Berlin, 2015), Springer Topics in Signal Processing Vol. 8.

[32]I. Ben Hagai, M. Pollow, M. Vorländer, and B. Rafaely, "Acoustic centering of sources measured by surrounding spherical microphone arrays," J. Acoust. Soc. Am. **130**(4), 2003–2015 (2011).
[33]E. Fernandez-Grande, "Sound field reconstruction using a spherical microphone array," J. Acoust. Soc. Am. **139**, 1168–1178 (2016).
[34]P. C. Hansen, *Discrete Inverse Problems: Insight and Algorithms* (SIAM, Philadelphia, PA, 2010), Vol. 7 of Fundamentals of Algorithms.
[35]J. J. Thomson, "On the structure of the atom: An investigation of the stability and periods of oscillation of a number of corpuscles arranged at equal intervals around the circumference of a circle; with application of the results to the theory of atomic structure," in *Philosophical Magazine* (Taylor & Francis LTD, Oxford, UK, 1904), Vol. 7, Issue 39, pp. 237–265.
[36]B. Rafaely, "Plane-wave decomposition of the sound field on a sphere by spherical convolution," J. Acoust. Soc. Am. **116**(4), 2149–2157 (2004).
[37]E. Williams and K. Takashima, "Vector intensity reconstructions in a volume surrounding a rigid spherical microphone array," J. Acoust. Soc. Am. **127**, 773–783 (2010).
[38]A. Granados, F. Jacobsen, and E. Fernandez-Grande, "Regularized reconstruction of sound fields with a spherical microphone array," Proc. Mtgs. Acoust. **19**, 055010 (2013).
[39]F. Jacobsen, G. Moreno-Pescador, and E. Fernandez-Grande, "Near-field acoustic holography with microphones on a rigid sphere (L)," J. Acoust. Soc. Am. **129**, 3461–3464 (2011).
[40]M. Nolan, E. Fernandez-Grande, and C.-H. Jeong, "Characterization of diffusivity based on spherical array processing," in *Proceedings of Internoise 2015*, San Francisco, CA (2015).
[41]E. Tiana-Roig, F. Jacobsen, and E. Fernandez-Grande, "Beamforming with a circular array of microphones mounted on a rigid sphere (L)," J. Acoust. Soc. Am. **130**(3), 1095–1098 (2011).
[42]E. Fernandez-Grande and A. Xenaki, "Compressive sensing with a spherical microphone array," J. Acoust. Soc. Am. **139**, EL45–EL49 (2016).
[43]M. Nolan, E. Fernandez-Grande, J. Brunskog, A. Richard, and C.-H. Jeong, "A wavenumber approach to characterizing the diffuse field conditions in reverberation rooms," in *Proceedings of the 22nd International Congress on Acoustics*, Buenos Aires, Argentina (2016).
[44]A. Xenaki, E. Fernandez-Grande, and P. Gerstoft, "Block-sparse beamforming for spatially extended sources in a Bayesian formulation," J. Acoust. Soc. Am. **140**(3), 1828–1838 (2016).
[45]R. Tibshirani, "Regression shrinkage and selection via the lasso," J. R. Statist. Soc., Ser. B **58**(1), 267–288 (1996).